International Journal of Applied Sciences: Current and Future Research Trends (IJASCFRT)

ISSN (Print) , ISSN (Online)

https://ijascfrtjournal.isrra.org/index.php/Applied_Sciences_Journal

Peaks Times of Transients in Transmission Systems based on Laplace Transform in Modal Coordinates

Mohamed Hamed[a*], Sara Nada[b]

[a]*Department of Electrical Engineering, Faculty of Engineering, Port Said University, Port Said, Egypt*

[b]*Department of Economics, Faculty of Economics & Political Sciences, Cairo University, Cairo, Egypt*

[a]*Email: hamed.mm@gmail.com,* [b]*Email: sara_nada14@hotmail.com*

Abstract

The current paper presents an analysis for the dependency of propagation self-parameters (propagation coefficient, attenuation factor and wave velocity) of some typical transmission lines (500, 330, 220, 110 kV) besides the distribution lines of 35 and 10 kV. The wave-mode parameters are deduced in modal coordinates (a, b, 0). Carson's equations for computation of frequency dependent parameters of overhead transmission lines are modified for the homogenous earth and the optimal number of terms of Carson's series is considered. The standard dimensions of towers are implanted, and the corresponding accurate propagation parameters of overhead transmission lines are obtained. Different arrangements of conductors for transmission lines are studied for the voltage levels of 500 and 220 kV. The mutual inductance and potential coefficient (mutual capacitance) of such arrangements are based (mirror effect). The time response for the first 5 peaks of transients for a long duration is intended and analyzed. The per unit system is accounted and the comparison is applied where the points of overvoltage are derived based on the convolution theorem and Laplace inverse structure. The voltages are computed for the specified points on the line (as SE, ¼ , ½ , ¾ , and RE) for considered voltage levels where a tailored comparison has been analyzed for the major parameters of propagation (Propagation Coefficient, Wave Velocity, Attenuation Factor). It is concluded that the time dependency is linearly with the rise of standard voltage of a line.

Keywords: Laplace Domain; Switching Transients; Tower Geometry Effect; Transmission Distribution Parameters; Wave Propagation.

---

* Corresponding author.

1. Introduction

Whatever, both resistances in the equivalent circuit of the system (transmission line, cable, winding, earth return path) induce a great loss against the sudden waves of transients so that both distortion and attenuation must be appeared to reduce theses sudden danger values [1-2]. Generally, there another type of transients which is known as the slow transients or the electrodynamic transients. The electrodynamic transits {in (□s)} is occurred due to switching or tripping conditions but the electrodynamic transients {in a few (ms)} are appeared due to the oscillation of generators in the united power network. Currently, it should be mentioned that the lightning surges are induced in extremely less than the electromagnetic switching processes {in (≤□s)} [3-4]. Otherwise, the lumped parameters electric circuit has a less time of electromagnetic transients relative to the transmission or distribution system as well as the electric network because of the distributed parameters of transmission system and that for the windings of either generators or transformers in the united electric network [5-6].

2. Problem Formulation

The current paper takes a homogeneous earth for the return path of voltages and currents during the electromagnetic transients. This will save to a great extent all connected equipment and devices as well as the components of the united network at all voltage levels. A few research has treated the effect of towers on the transients where the line will be nonuniform. There are 3 different concepts for the consideration effect of tower transients as [7-8]:

i- The Bewley Lattice diagram representing the travelling waves (lossless reflecting and refracting) method according to the places of towers along each line [8].

ii- The sectionalization of tower into (L) multi-series section (usually dissimilar) where this concept is the same as (p) and (T) equivalent circuits. Both Differential Equations for inductance currents and capacitance voltage are simulated mathematically, for the nonlinearity (as corona), to be solved [9].

iii- The characteristic Equation for the tower propagation parameters in Laplace complex domain (Closed Form) based on the specified tower locations (including the tower footing resistance if found) to be solved analytically. The inverse Laplace transformation could be implemented for the return to the original time domain [6, 10].

3. Theoretical Analysis

Generally, The study of travelling waves leads to the exact determination of voltages and currents through different points along the specified line. This is the starting point for the insulation level across the transmission system not the line alone. It is a starting point for the analysis of electromagnetic transients while the second face may be appointed as the overvoltage which is occurred either internally due to switching processes or externally with lightning surges. It is the first step for the analysis of insulation coordination for the power system totally [11-12].

3.1. Mathematical Base

There are some different approaches tried to regulate the parameters of a power system generally. Others went to transmission lines or even to change the concept of transmission, but the final practical solution requires more effort. The switching transients depends on the parameters of the system where the ground return effect plays a key role. The earth will be considered as a homogenous for simplicity and so, the Carson concept would be applied. Otherwise, the capacitance is taken as a constant without any ground effect while the frequency dependent parameters are introduced. The self-capacitance will be (C_s) and the mutual will be (C_m). Then, the impedance matrix [Z] would be taken in the usual two parts of the resistance matrix [R] and the matrix of reactance [X] as [7, 11]:

$$[Z] = [R] + j\,[X] \qquad (1)$$

This Equation may be tailored into the original elements where the resistance matrix (R) would be expressed through the conductor resistance (R_c) besides the ground resistance (R_g) in the matrix form:

$$[R] = \begin{vmatrix} R_c+R_g & R_g & R_g \\ R_g & R_c+R_g & R_g \\ R_g & R_g & R_c+R_g \end{vmatrix} \qquad (2)$$

Similarly, the matrix of inductive reactance (X) may be simply expressed as a function of the Self-inductance of a line (L_s) besides the Mutual inductance (L_m) according to the angular frequency (w) by:

$$[X] = jw \begin{vmatrix} L & M & M \\ M & L & M \\ M & M & L \end{vmatrix} \qquad (3)$$

The current paper analyzes both systems of transmission at voltage levels 500, 330, 220, 110 kV and distribution levels 35, 10 kV representing the united network to discover the propagation characteristics for a system within electromagnetic transients. The overall geometry of phases is based on the standard towers [9]. Universally, the transient characteristics depend on the main parameters of transmission systems because they come from the geometry of phases. Thus, the geometry allocation of phases will reflect the overall behavior in the frequency domain of internal transients. Additionally, the voltage levels of distribution and transmission systems would control the generalization process to be stamped. This may stress on the presented work according to the performance of propagation parameters within switching transients in power system. After that, a pattern for wave propagation along and across a line (and even with tower effect) can be computed simply while the statistical study may assist [8]. Chiefly, voltage V(x) and current I(x) at a point x (measured from the sending end) of the line having a length of l, would be expressed in the matrix form:

$$\begin{aligned} -\partial/\partial x\,[V(x)] &= [Z]\,[I(x)] \\ -\partial/\partial x\,[I(x)] &= [Y]\,[V(x)] \end{aligned} \qquad (4)$$

Applying the Sylvester theorem, the voltage V(x) at a point x may be obtained as [7]:

$$V(x) = \tfrac{1}{3} \{Ch\ \gamma_1(l\text{-}x)\ [M_1] + Ch\ \gamma_2(l\text{-}x)[M_2])\}[V(l)]$$
$$+ \tfrac{1}{3} \{Z_1\ Sh\ \gamma_2(l\text{-}x)\ [M_2] + Z_2\ Sh\ \gamma_1(l\text{-}x)\ [M_1])\}[I(l)] \quad (5)$$

The voltage {V(l)} and current {I(l)} are the values at the receiving end of the line. the elements of Equation may be defined by the first mutual matrix [M_1]:

$$[M_1] = \begin{vmatrix} 1 & 1 & 1 \\ 1 & 1 & 1 \\ 1 & 1 & 1 \end{vmatrix} \quad (6)$$

The second mutual matrix [M_2] becomes:

$$[M_2] = \begin{vmatrix} 2 & -1 & -1 \\ -1 & 2 & -1 \\ -1 & -1 & 2 \end{vmatrix} \quad (7)$$

Additionally, the characteristic impedances (Z_1 & Z_2) can be stated through:

$$Z_1 = \sqrt{\frac{R + p\ (L - M)}{p\ (C - C_m)}}$$
$$Z_2 = \sqrt{\frac{R + 3R + p\ (L + 2M)}{\{\ p\ (C + 2\ C_m)\}}} \quad (8)$$

Otherwise, the current I(x) at a point x, depending on the surge impedance (Z_c), goes to:

$$[I(x)] = \{Sh\ \gamma_2(l\text{-}x)\ [Z_c]^{-1}\ [v(l)] + Ch\ \gamma_1(l\text{-}x)\ [I(l)] \quad (9)$$

3.2. Modal Coordinates {(α), (β), (0)}

The replacement of the matrix of propagation coefficient by a multi term Equation according to Sylvester theorem will simplify the obtained expression for the propagation coefficient (γ):

$$[\gamma] = \tfrac{1}{3}\ \lambda_1\ [M_1] + \tfrac{1}{3}\ \lambda_2\ [M_2] \quad (10)$$

The included roots of characteristic equation for the propagation coefficients variable may be specified as:

$$\lambda_1^{\,2} = \gamma_1 + 2\gamma_2$$
$$\lambda_2^{\,2} = \lambda_3^{\,2} = \gamma_1 - \gamma_2 \quad (11)$$

Then, the propagation coefficient becomes:

$$e^{[\gamma]x} = \tfrac{1}{3}\, e^{\lambda_1 x}\ [M_1] + \tfrac{1}{3}\, e^{\lambda_2 x}\ [M_2] \qquad (12)$$

The analysis would be more complicated for either non-transposed or partially transposed lines in the Laplacian domain (closed form) and so the final formula can be solved in the wave-mode coordinates. The distribution networks play a vigorous role in the processes of operation and many papers were analyzed this system. The modal technique is a simple procedure to solve the problem in the complex plane where the main parameters may be applied in each wave-mode {(α), (β), (0)},, individually. The modes are isolated channels without any mutual relationship between them and they defined as {(α), (β), (0)}.

The propagation coefficient can be estimated mathematically in each channel to obey:

$$e^{[\gamma]x} = \frac{(\gamma_\beta-\gamma)(\gamma_0-\gamma)}{(\gamma_\beta-\gamma_\alpha)(\gamma_0-\gamma_\alpha)} e^{\gamma_\alpha x} + \frac{(\gamma_\alpha-\gamma)(\gamma_0-\gamma)}{(\gamma_\alpha-\gamma_\beta)(\gamma_0-\gamma_\beta)} e^{\gamma_\beta x} + \frac{(\gamma_\alpha-\gamma)(\gamma_\beta-\gamma)}{(\gamma_\alpha-\gamma_0)(\gamma_\beta-\gamma_0)} e^{\gamma_0 x}$$

(13)

This formula can be expanded in the modal coordinates as:

$$e^{[\gamma]}_{x} = e^{\gamma_\alpha x}\begin{vmatrix}10\\0\\00\\0\\00\\0\end{vmatrix} + e^{\gamma_\beta x}\begin{vmatrix}00\\0\\01\\0\\00\\0\end{vmatrix} + e^{\gamma_0 x}\begin{vmatrix}00\\0\\00\\0\\00\\1\end{vmatrix} \quad (14)$$

On the other hand, the attenuation factor plays a distinguished role in the limitation of overvoltage since it is representing the effective part of the propagation process. The maximum ratio is corresponding to the higher voltage class. The derived Equations will be more complicated for the non-transposed lines in the Laplacian domain (p) and so the initial formula can be solved in modal coordinates. Also, the distribution networks play a vital role in the operation conditions analyzed before. Many methods are known for the transient calculations and the wave-mode propagation method will be selected since it is a valid expression for either transposed or non-transposed lines. It depends on the transformation matrix [T], which takes the form:

$$[T] = \begin{vmatrix}1 & 1 & 1\\0 & -B & A\\-1 & 1 & 1\end{vmatrix} \qquad (15)$$

The appeared elements of the transformation matrix can be referred to the Clark Components for the symmetrical lines (A = 1 & B = 2) but the coefficients in this Equations are (A = 1.2 & B = 1.8) for the

asymmetry (non-transposed) lines [7, 13, 14].

If the basic differential Equations are specified to the modal coordinates individually, both expressions become:

$$-\partial/\partial x\,[V(x)_{\alpha,\beta,0}] = [Z]\,[I(x)_{\alpha,\beta,0}]$$
$$-\partial/\partial x\,[I(x)_{\alpha,\beta,0}] = [Y]\,[V(x)_{\alpha,\beta,0}] \qquad (16)$$

Both voltage V(x, p) and current I(x, p) at point x in modal coordinates will be:

$$\begin{aligned}[V(x,p)]_{\alpha,\beta,0} &= [Ch\ \gamma(l\text{-}x)]_{\alpha,\beta,0}\,[V(l,p)]_{\alpha,\beta,0} \\ &\quad + [Sh\ \gamma(l\text{-}x)]_{\alpha,\beta,0}\,[Z_c]_{\alpha,\beta,0}\,[I(l,p)]_{\alpha,\beta,0} \\ [I(x,p)]_{\alpha,\beta,0} &= [Sh\ \gamma(l\text{-}x)]_{\alpha,\beta,0}\,[Z_c]^{-1}_{\alpha,\beta,0}\,[V(l,p)]_{\alpha,\beta,0} \\ &\quad + [Ch\ \gamma(l\text{-}x)]_{\alpha,\beta,0}\,[I(l,p)]_{\alpha,\beta,0}\end{aligned} \qquad (17)$$

These Equations depend on the transformation of the phase system into another one, which is known as the wave-mode system [7]. This means that the wave modal concept has three isolated modes without any mutual effect between them as this can be reached through the mathematical theorem of Eigen values and Eigen vectors. It should be noted that the transformation matrix represents the Eigen vectors for the system. A special program is used for the calculations of parameters in wave-modes or the transients and modified to measure the statistical values as presented here. The application of parameters in modal axes is based on the matrix Equation:

$$[E] = [T]\,[Z_c\ Ch\ \gamma l\ /\ Sh\ \gamma l]\,[T]^{-1}[I(0)] \qquad (18)$$

Normally, these Equations must be referred to the voltage source at the sending end (SE) instead of the voltage at receiving end (RE). Then, a simplified formula for voltage V(x, p) and current I(x, p) may be formulated by:

$$[V(x,p)]_{\alpha,\beta,0} = [Ch\ \gamma x]_{\alpha,\beta,0}\,[V(0,p)]_{\alpha,\beta,0} + [Sh\ \gamma x]_{\alpha,\beta,0}\,[Z_c]_{\alpha,\beta,0}\,[I(0,p)]_{\alpha,\beta,0}$$

$$[I(x,p)]_{\alpha,\beta,0} = [Sh\ \gamma x]_{\alpha,\beta,0}\,[Z_c]^{-1}_{\alpha,\beta,0}\,[V(0,p)]_{\alpha,\beta,0} + [Ch\ \gamma x]_{\alpha,\beta,0}\,[I(0,p)]_{\alpha,\beta,0} \qquad (19)$$

3.3. Laplace Domain

It is significant to state that the voltage source E(p) differs from the voltage at the sending end V(0, p) because

of the internal impedance (L_{supply}) of the supply. This may be written in the mathematical expression:

$$[V(0, p)]_{\alpha, \beta, 0} = [E(p)]_{\alpha, \beta, 0} - p\,[L_{supply}] \qquad (20)$$

So, the voltage may be formulated through the transformation matrix:

$$[V(x, p)]_{\alpha, \beta, 0} = \frac{[\mathrm{Ch}\ \gamma(l\text{-}x) / \mathrm{Sh}\ \gamma l]_{\alpha, \beta, 0}\,[E(p)]}{B\,[Z_c]_{\alpha}\,[\mathrm{Ch}\ \gamma(l\text{-}x)/\mathrm{Sh}\ \gamma l]_{\alpha}} + A\,\frac{\mathrm{Ch}\ \gamma(l\text{-}x)}{\mathrm{Sh}\ \gamma l}\,[Z_c]_{\beta} \qquad (21)$$

Therefore, voltages in phase coordinates can be determined numerically according to the convolution theorem as:

$$\begin{aligned} V_a(x,p) &= AV_{\alpha} + B\,V_{\beta} + (A+B)\,V_0 \\ V_a(x,p) &= AV_{\alpha} + B\,V_{\beta} + (A+B)\,V_0 \\ V_c(x,p) &= AV_{\alpha} + B\,V_{\beta} - (A+B)\,V_0 \end{aligned} \qquad (22)$$

Similarly, the formulation of currents in phase coordinates can be deduced through the convolution theorem and the Laplace Inverse. The software is based on the FORTRAN IV where it is scientifically used the Laplace domain and the convolution theorem for the inverse Laplace. The main parameters (input data) are the line dimensions and the time interval of T = 0.23 ms but the total time of 32.2 ms is considered for 140 points within the time interval. The per unit system is applied for the computational processing to maximize the accuracy of results. The overvoltage is accounted for different points along the line length of (l) as SE, ¼, ½, ¾, and RE where SE and RE represent the sending end and the receiving end, respectively. The data of study lines are listed in Table 1.

Table 1: The specified line lengths

kV	500	330	220	110	35	10
Length, km	500	300	200	100	30	10

3.4. Overvoltage Times

The paper is directed to the peaks of transients where 5 peaks are deduced within analysis. The results for the number of points in each point above the standard voltage are accounted as plotted in Figure 1. Globally, a power system operates under a steady-state condition where transients and oscillation as well as the system drop are a faulty case. However, these transients are normally occurred due to either disturbances (switching) or sudden short-circuits or even disasters of lightning strike for a very extremely short time. Figure 1 illustrates

that the longer time for overvoltage presence is appeared always at the ¾ of the line length for all studied levels of voltage in the transmission system, but it is constant along the distribution level along each line (35 and 10 kV). It is also seen that the rate of rise of time is greater for the higher voltage in the transmission system. The time distribution of overvoltage points for the full length of lines (RE) is calculated and the results are plotted in Figure 1 (The second drawing). Both transmission and distribution systems are introduced for the computations where the results show that number of points above the nominal voltage during a specified time are presented for the lengths indicated on the graph for each voltage. The transmission voltages are 110, 220, 330, 500 kV for lengths of 100, 200, 300, 500 km, respectively, when the distribution voltage is represented for voltages 10 and 35 kV.

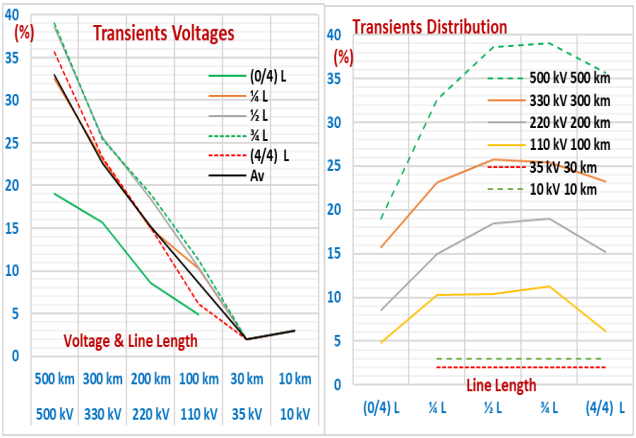

Figure 1: The overvoltage times for lines & at RE %

The average performance for these results is computed as drawn in Figure 2 (a). It is in the percentage scale where the maximum value is going always towards the higher voltage. The spread average is linear without any fluctuations while the voltage level 500 kV stands at 32.97%. Since the distribution characteristics are steady without any change along the duration or the type of lines and voltages, the contents of time for the line voltages may be estimated for a few points (SE, ¼ *l*, ½ *l*, ¾ *l*, RE) along each line. The results are plotted in Figure 2 (b) for the rise of overvoltage along the lines in transmission systems in per unit scale.

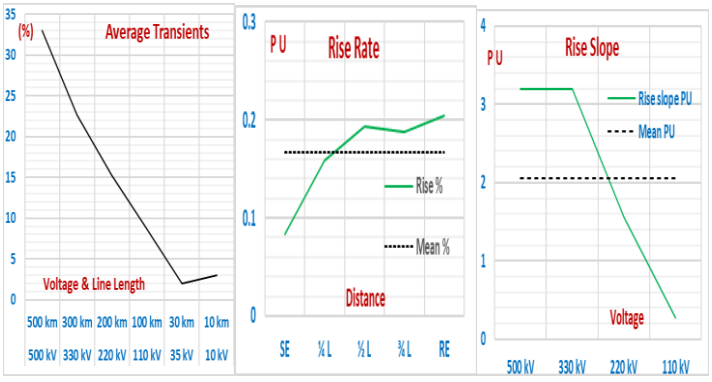

Figure 2: The time distribution of overvoltage points (a) at RE (b) overvoltage rise (c) P U rise slope

It is seen that the overvoltage is going up toward the end of the line in the transmission system but there is a direction for the rise of overvoltage. This may be defined across the rate of rise each so that the deduced rise slopes are indicated in Figure 2 (c).

4. Overvoltage Peaks

Five peaks are accounted for a switching on process for each line where the return earth effect is inserted based on Carson formulation. The frequency dependency is parameters is included with a homogeneous earth return effect where the Laplace transform, and the convolution theorem are considered [7, 11]. It is seen that the total number of points above the unity is higher for the higher voltage while the characteristics give a linear down with voltage. It is a linear relationship approximately. The number of points is corresponding to the time under pressure which press on the insulation level of the lines. It should be remarked that the first peak has a higher voltage than the next and so on. The time assumed the summation of time for each peak although the value is not constant for all points. The research measures the total time above the nominal in general.

4.1. First Peak

Figure 3 indicates that the time dependency first peak of the oscillation of voltage curve for different points along the line length has the same rise shape of the total summation curve. It is also seen that the higher voltage is the greater time for the duration in the first peak, but it is constant and low for the two lines in the distribution system. It is remarked that an oscillation in the shape appeared for the voltage 110 along the line because of the reduction in the voltage duration at the middle point of the line. Secondly, the RE and SE are approximately the same relative to the first peak while the RE is always higher for the voltages above.

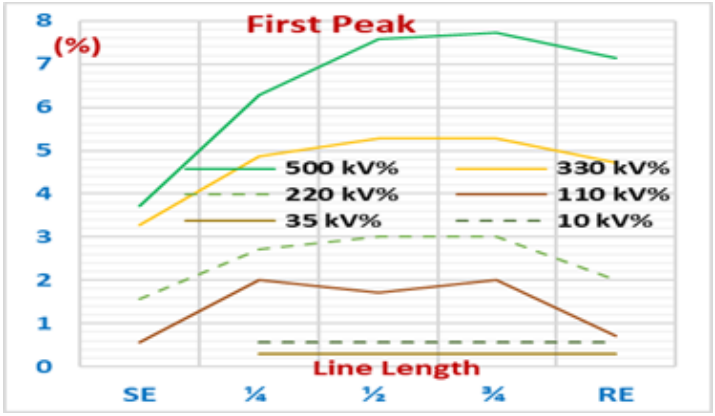

Figure 3: The characteristics of the first peak.

4.2. Second & Third Peaks

High drop for the time of second peak is appeared in Figure 4 for the voltage 220 kV while the mean duration is 2.6%. All other curves say the same as for the first peak.

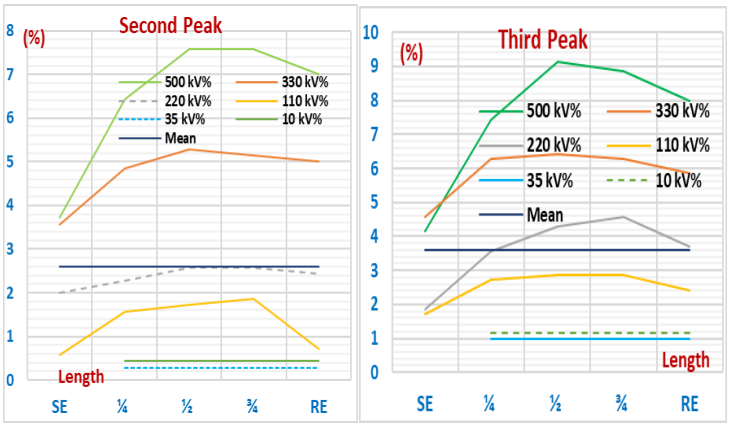

Figure 4: The characteristics of the 2nd and 3rd peaks.

The third peak as shown in Figure 4 also gives another characteristic relative to the first and second peaks where the SE points for 220 and 110 kV are closed to each another. Also, the SE of 500 kV goes down than that for 330 kV while the RE keeps the same shape relative to the SE for all lines. Contrary, the distribution system is still idle for all calculated points and cases.

4.3. Fourth / Fifth Peaks

The fourth peak according to Figure 5 get a modified shape for the duration of overvoltage where a smooth slow rise is initiated for all lines in the transmission system. This slow began at the middle point of the line for all except 110 kV which started before (at ¼) of the line length.

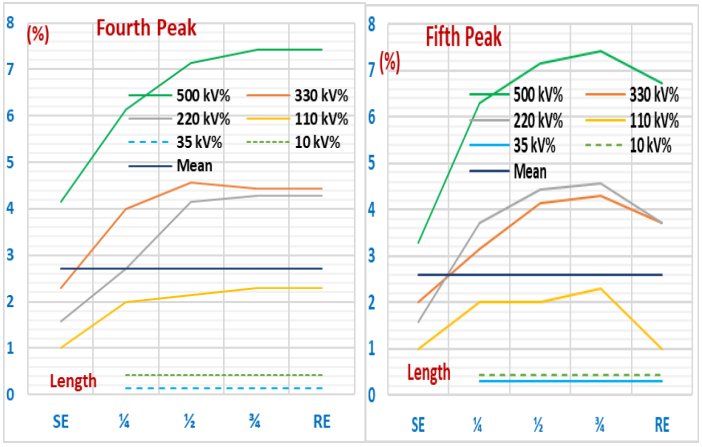

Figure 5: The characteristics of the 4th/5th peaks.

The overvoltage duration for the fifth peak has the same values for the fourth but the characteristics goes to the first and second peaks (Figure 5).

4.4. Total Time dependency

The assembling of all results of all overvoltage points, in Figure 6, where all rise rates for all peaks are the same (about 0.6 PU) at 500kV. A difference began at the level of 330 kV while the 4th peak becomes the highest rate with a continuous maximum rate for all next voltages. The other rates oscillated under the rate of 4th peak. Otherwise, the average of rise rate is the same for all levels of voltage individually. This is proved according to the results listed in Table 2.

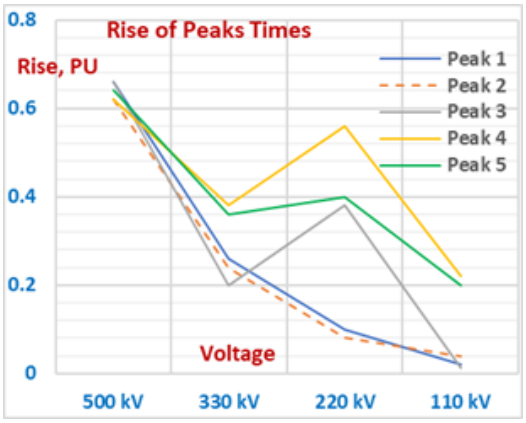

Figure 6: The development of peaks times of overvoltage in transmission systems (P U)

Table 2: The mean value for the peak's times

kV	500 kV	330 kV	220 kV	110 kV
Peak Times1	0.26	0.26	0.26	0.26
Peak Times2	0.245	0.245	0.245	0.245
Peak Times3	0.313	0.313	0.313	0.313
Peak Times4	0.445	0.445	0.445	0.445
Peak Times5	0.4	0.4	0.4	0.4

5. Statistical Analysis

Principally, the electrical state of the line during switching will not reach the steady state instantaneously. Usually, elapses between start and final steady states because of the internal transient phenomenon within a very short time in the rate of □s. so, this case is defined as the electromagnetic transients or internal overvoltage. When the long circuits such as the transmission line this case becomes more important to save the components of the circuit against the overvoltage induced. The switching processes are increased with the long transmission line because of its distributed parameters. Contrary, the electric circuit are more defined and accurately

determined while the distributed parameters of a line send the problem to another mode to be solved. For transmission lines, the voltage wave travels along the line till its end although the surges of lightning strokes move in the same way. The voltage wave is always accompanied by a current wave where both waves travel at the light velocity [12, 15]. Moreover, the variation of time domain length can be examined by different intervals, but the given paper assumed an interval of 0.23 ms for 700 ms. The low voltage 10kV gives slowly decrease with time duration while it is practically constant for 35 kV. Also, the overall average voltage for studied lines is decreased due to the presence of steady state period inside the process of calculations.

5.1. Standard Deviation (s)

The standard deviation is a vital factor for the statistical studies where the statistical points above the standard voltage may be evaluated according to the standard deviation. The results are plotted in Figure 7 while different shapes are received for all lines in either transmission or distribution systems.

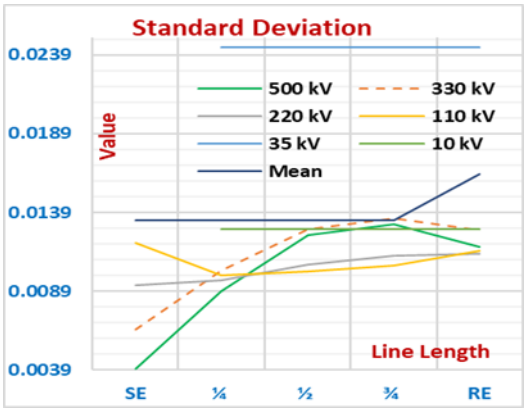

Figure 7: The standard deviation for higher points of overvoltage (V > 1) at different distances of the line.

The populations for the readings of overvoltage above the unity are inserted totally in the computation of standard deviation. The accounted overvoltage is the values for the different voltage levels as well as for the spreading along the line as (SE, ¼ *l*, ½ *l*, ¾ *l*, and RE) when all results are sketched in Figure 7. The distribution network is introduced besides the transmission system. It is seen that the 35 kV level stands alone above all while the average value for the resulted standard deviation is located near all readings away from the level 35 kV. This remark may be referred to the tower dimension of 35 kV level. Similarly, the overall mean value for all studied standard transmission and distribution lines is 0.01138 while the standard deviation for the transmission lines is fluctuating between 0.0039 for 500 kV at the SE and 0.01338 for 330 kV at ¾ of the line.

5.2. Mean Value

Specifically, the propagation properties of transmission lines should be formulated by the distributed parameters of a line so that the control of these parameters can reach a good statement. The parameters of transmission lines at the steady state condition differ completely from the same at the electromagnetic durations. This difference comes from the asymmetry of parameters individually where the parameters of each phase diverse from the

other two.

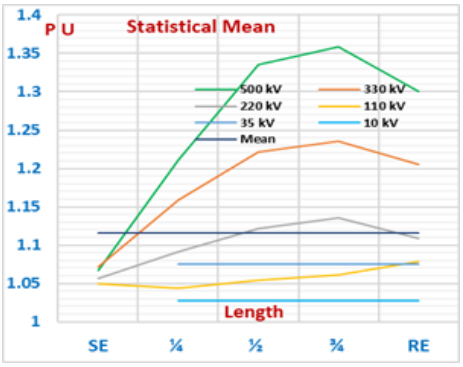

Figure 8: The mean value for higher points of overvoltage (V > 1) at different line distances.

Additionally, the mean value (corresponding to the results of standard deviation) must be extracted when the results are graphed in Figure 8 for all studied lines. The mean value for all readings in the studied model is 1.1159 in per unit system while the mean value is constant for both lines in the distribution system. The mean value is the highest at ¾ of the line length for all transmission lines except the line 110 kV.

6. Wave Parameters

Then, the symmetrical assumption will give wrong results although the wires are beside each other for a long distance. Mainly, this problem may be partially solved depending on the transposition concept but contrary this is difficult for the transients' durations. If the propagation characteristics are the target, the major parameters of the line must be inserted. These parameters may be divided into two parts while the first will contain the basic three parameters (resistance, inductance, capacitance). These parameters are distributed along the line length symmetrically although for transients they become different. Secondly, the propagation parameters may be required to explain the performance of such lines during the transients' processes [8, 12].

6.1. Propagation Factor (g)

The second part is the return parameters where the earth is the return path which is usually inequal for all contents. The first assumption is the consideration of the earth as a homogeneous (symmetrical earth parameters) although each parameter would be dissimilar. Therefore, the Carson mathematical simulation for the earth could be applied for the present analysis where the propagation parameters for the line can be estimated correctly. These propagation parameters may be concentrated in the propagation coefficient (g), the attenuation factor (d) and the wave velocity (v). Additionally, the time effect may be introduced for the evaluation of the effect of time of overvoltage (time-harmonic) on the insulation coordination when the reflection coefficient for Lattice diagram has no meaning because of the applied Laplace method. The propagation coefficient is varied in these coordinates where per unit system is considered. The frequency presence inside the processes of transients may reach 60 kHz due to the HF loads and interference with electromagnetic fields. The power frequency 50 Hz at zero-mode position is taken as the reference (unity value)

and then its value is illustrated for studied voltage levels. The coefficient is increasing with frequency in zero-mode while it is decreased in other channels. The maximum ratio of this coefficient is appeared for 110 kV, where the 35 kV distribution lines approaches the case of 500 kV. The results of calculations are sketched in Figure 9 for all investigated lines but in the wave-modal coordinates (a, b, 0) based on the Laplace method [7]. The drawing proves that the propagation coefficient is higher for the lower voltage within the transmission system. It should be mentioned that the frequency of 60.05 kHz is added for the main program where the margin of frequencies become (50 Hz-60.05 kHz) instead of the original margin of (50 Hz-50 kHz) to cover the over frequencies inside the transients' processes.

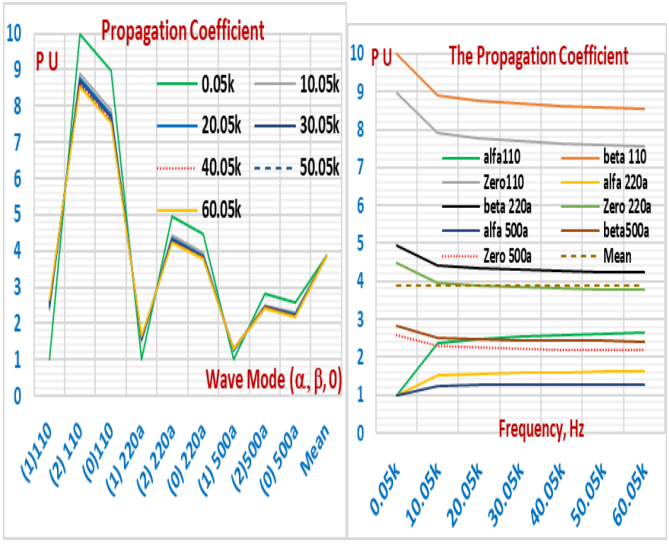

Figure 9: The P U dependency of (g) on the frequency in modal coordinates (a, b, 0).

Calculations of the new wide margin of frequencies leads to some modification in the wave-modal parameters as printed in Figure 9 where parameters have a very slowly increase in all wave-modal coordinates (a, b, 0). The low frequency band has a visible change up to the 10 kHz when it is increasing for the parameters in 1st wave-mode (a) for all lines. Contrary, these parameters are decreasing in both the 2nd wave-mode (b) and the zero wave-mode (0). Accordingly, the chosen 4 lines are tested by comparison for the propagation coefficient when the test results are plotted in Figure 9. The results are given in the wave-modal coordinates (a, b, 0) while a difference is appeared for both levels of voltage.

6.2. Wave Velocity (v)

When a transmission line is energized (connected to a voltage source), the line end will not instantly energized. This is occurred because the electricity moves at the light velocity (3.108 km/s). Normally, the waves travel along the line at a modified wave shapes and magnitudes momently when this change is specified by the distortion (attenuation) factor due to the presence of line resistance as well as the resistance of earth return during the transient processes [8].

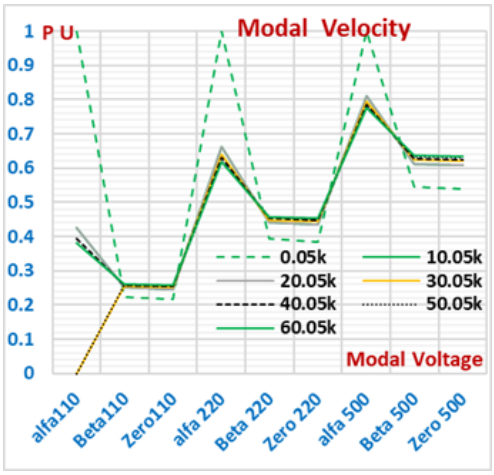

Figure 10: The dependency of **(*v*)** for different levels of voltage in modal coordinates (a, b, 0).

The frequency characteristics are deduced as drawn in Figure 10 while the results are given in modal coordinates (a, b, 0). Figure 10 presents the wave velocity in each wave-mode (a, b, 0) for the chosen voltages (110, 220, 500 kV) as transmission system. The wave velocity in the first mode (a) is the higher but it decays from the light velocity with the frequency rise. Contrary, the velocity is increasing in the wave-modes (b, 0) in the range of 0.25, 0,4, 0.6 for the voltages 110, 220, 500 kV, respectively. These values are referred to the light velocity since the first wave-mode (a) has lower resistance relative to the others. The total mean value is 0.515 for the wave velocity in the system which may be defined as shown in Figure 10.

6.3. Attenuation Factor (d)

Since the accurate estimation for the insulation coordination depends on the good analysis for the main parameters of the line which has distributed parameters. So, the current paper treats the fundamental propagation parameters in three values as the wave velocity, the attenuation factor and the propagation coefficient are analyzed. The frequency dependent for parameters is considered while the mirror effect (as a reflection for the topology) is accounted. Moreover, the earth return effect is introduced according to the mathematical formula of Carson. Since the single-frequency simulation would not be appropriate, the long term of frequency presentation could be implemented. The attenuation factor is the important element in the transients' processes because it is the breaking force for the voltage development. Therefore, the attenuation factor must be resolved for illustration. It has been estimated in the wave-mode coordinates (a, b, 0) as given in Figure 11 where has the highest value for the wave-mode (a) for all voltages. Similarly, the other two wave-mode (b, 0) have the same performance of the first (a). The attenuation factor (Figure 11) is increased individually in each wave-mode (a, b, 0) with the higher transmission voltage for all frequencies when the low frequency takes less attenuation value. The zero wave-mode (0) has the less attenuation as proved in Figure 11.

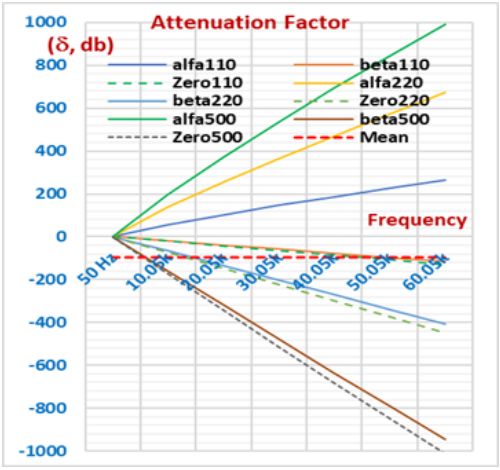

Figure 11: The dependency of (d) for voltages in the modal coordinates.

The attenuation factor (Figure 11) is vital for stopping the peaks where its dependency (in the wave-modal coordinates a, b, 0) is linear for all cases. These values are given for the supposed frequencies which means a higher attenuation for higher harmonics where it is purely positive (high value) in the 1st wave-mode (a). The general mean value for all data on the graph is -95.22 db while the attenuation in each wave-mode (a, b, 0) is highly rising towards more attenuation effect.

6.4. Tower Dimensions

Globally, there are different types of towers for each voltage of either transmission or distribution systems although there are also, a few of dimensions for each type of towers. Consequentially, the results may vary according to the used dimension so that a current comparison would be treated simply to illustrate this phenomenon. The effect of tower dimensions is appeared in the results of as plotted in Figure 7 for the calculated standard deviation of all. The 35 kV dimension gave a high value than all others either above (500, 220, 1110 kV) or less as 10 kV. Continuously, the paper is simply simulating a comparison procedure for the three fundamental propagation parameters through two dimensions for two different voltage levels as listed in Table 3.

Table 3: The selected dimensions for overhead lines.

Voltage	Height a	Spacing a	Height b	Spacing b
220 kV	8	6	8	5
500 kV	12.54	13	13.2	11

Then, a specific study for comparison would be presented based on the data of Table 3.

i- Propagation

Since there are different dimensions for towers of the same voltage, the current research dealt with this into two voltage levels (220 and 500 kV). Two different dimensions for standard towers are selected as listed in Table 3. The wave-mode (a) indicates that the case b of dimensions 220 kV is higher than the case a, referring to Figure 12 but both cases of 500 kV are approximately the same. The second wave-mode (b) proves that the case b of dimensions 220 kV is more relative to the case a while case b is higher for 500 kV than case a (in less ratio). Finally, the zero wave-mode (0-mode) illustrates the same conclusion of wave mod (b). This concludes that the dimension is important for the propagation coefficient so that a recommendation can be declared.

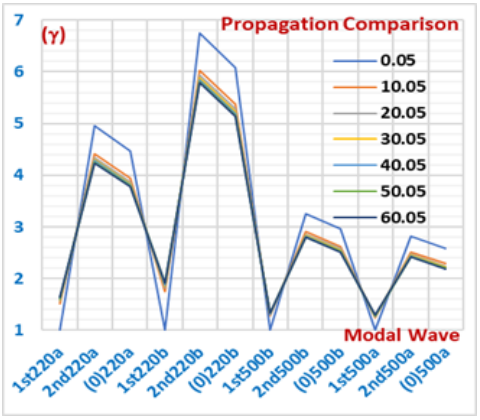

Figure 12: The frequency dependent of (g) for comparison between standard dimensions of towers (220 & 500 kV) in modal coordinates (a, b, 0).

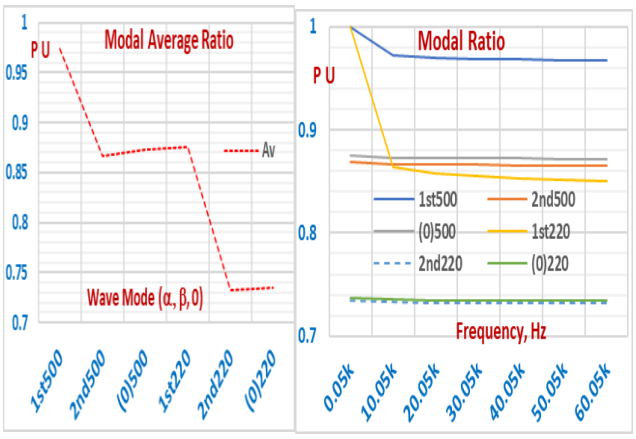

Figure 13: The average of (g) for compared voltages (220 & 500 kV) in modal coordinates (a, b, 0).

Consequentially, the average value of propagation coefficient would be derived as graphed in Figure 13 according to each wave-mode (α, β, 0) where always the wave-mode (α) is the higher and the wave-mode (β) is the lower for both voltages. The zero-mode closes to the wave-mode (β) but higher a little. Specifically, the propagation coefficient in the modal coordinates (α, β, 0) for the 500 kV as (0.9733, 0.8661, 0.8725) is higher than the corresponding for 220 kV (0.8758, 0.7325, 0.7353), respectively.

Therefore, the parameters of the system must be evaluated. Two limits (upper and lower) are indicated where both channels {1st (α) & 2nd (β)} have a higher value than that for the zero wave-mode (0). It is increasing with voltage level in the two modes, but it is a constant in the zero-mode

ii- Velocity

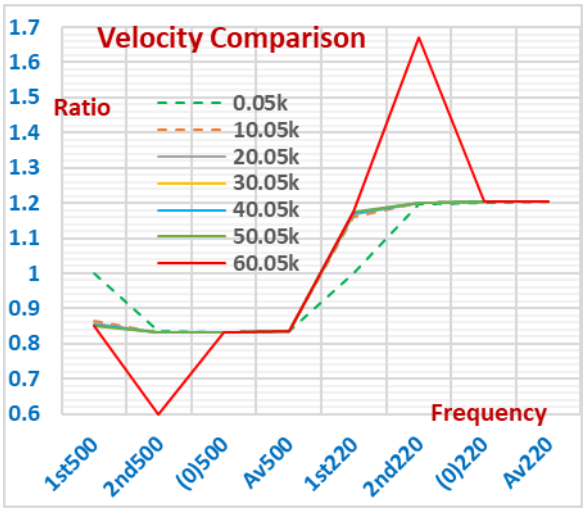

Figure 14: The velocity function for compared voltages (220 & 500 kV) in modal coordinates.

Similarly, the comparison between different dimensions of the towers may be introduced based on the data of Table 3 and the results are dropped in Figure 14. The results are the ratio of velocity of the case a to the velocity of the case b. Wave velocity in all wave-modes (a, b, 0) for 220 kV is higher than that for 500 kV. On the other side, the ratio in the wave-mode (a) is increasing for the 220 kV case although it is decreasing for the 500 kV. The other two modes (b, 0) have a constant velocity except at the 60 kHz condition. The average dependency of (v) for compared voltages (220 & 500 kV) in modal coordinates (a, b, 0) is given in Figure 14.

iii- Attenuation

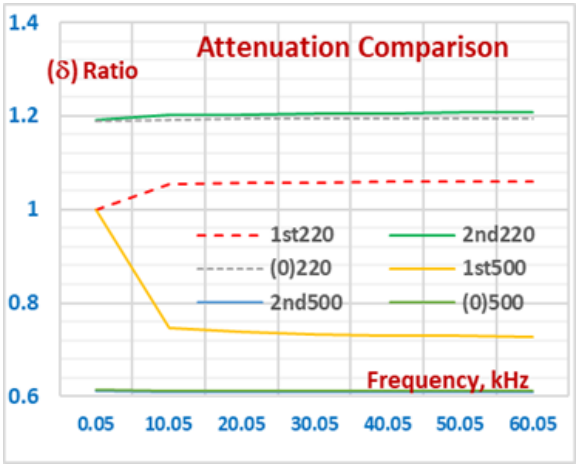

Figure 15: The dependency of (d) for compared voltages (220 & 500 kV) in modal coordinates.

Notably, the tower surge impedance may be added to the line characteristic impedance mathematically to reach the actual representation for the overhead transmission lines. It should be noted that the tower surge characteristic has higher effect in the cases of lightning strikes where it plays a vital role in the damping

coefficient besides the mutual induced values across. Accordingly, towers resonance response may be deduced when the lightning strikes [9]. Similarly, the comparison for the attenuation factor is obtained as drawn in Figure 15 where the ratio of the tower type (a) to the tower of type (b) is deduced as printed in Figure 15.

However, the wood towers prove a lower attenuation so that its value for 35 kV towers may exceed that for the 110 towers.

7. Discussion

An analysis for the current research may be required for the clarification of the subject. Chiefly, the first item of work is mainly the asymmetry configuration of conductors due to their allocations along a long distance from SE to RE points. This asymmetry appears in all overhead lines without exception but practically, the companies try to balance the difference between phases by installing the transposition towers. Since these towers are very expensive, a transposition cycle is considered for this process. This means that the total line length is divided into three parts or 6 or 9, etc. The best number is the larger (9 or more) although the lowest number (3) is always the selected because of the economic consideration. This clarifies that the line parameters will not be symmetry exactly so that a semi-symmetry will be injected instead. This situation is real for the steady state conditions (operation) but it becomes asymmetry totally for the transients conditions (switching processes and lightning strikes). Firstly, the current paper works on this transient case so that the symmetrical lines are not real. Most papers treat such problem as symmetry while others consider the asymmetry configuration. This last part of research always depends on either the partition of the lines into several p or T equivalent circuits or on the Fourier Analysis in the time domain. Both are limited due to the multi term of series or equivalent circuits. Contrary, the present work depends on Laplace domain in the frequency domain, which is an exact solution, mathematically. Secondly, the modal analysis depends on the wave propagation on the wires of conductors in the modal coordinates (a, b, 0) where the (0) mode has a lowest velocity and highest impedance. The paper emphasizes on propagation coefficient (wave velocity and attenuation factor) for decaying the travelling waves on the conductors. Thirdly, the paper concentrates on danger part of voltage during transients so that the values above unity may be the danger. So, the peaks of voltage (above the nominal unity) are considered for the analysis through the propagation coefficient.

8. Conclusion

From the results and analysis of the current paper, it can be concluded that:

1- The peaks times for the distribution network is invisible so that it can be neglected.

2- The insulation level of overhead lines in transmission systems should be integrated with distance towards ¾ of the line length.

3- The average rise of peaks times is independent on the voltage level.

4- The rise of peaks times for first peak only is increased with voltage level rise.

5- The dependency of wave attenuation is purely linear with frequency.

6- A widespread dimension for all towers must be introduced for the generalization of transients' performance in either transmission or distribution systems.

7- The modal analysis is a clear way for comparison between towers or lines.

8- The peaks times are important for the protection of the insulation level against damage.

9- The wave velocity in the zero-wave mode is lower.

Reference

[1]. D. Bellan & G. Superti-Furga (2018): Space-vector state-Equation analysis of three-phase transients. J. Electr. Syst., 2018, Vol. 14 (188–198).

[2]. D. Bellan (2019): Analytical approach to transient solution of single-line and double-line faults in three-phase circuits, Int. J. Circuits Syst. Signal Process, 2019, Vol. 13 (647–653).

[3]. F. Plumier, P. Aristidou, C. Geuzaine, T. Van Cutsem (2016): Co-simulation of electromagnetic transients and phasor models: A relaxation approach. IEEE Trans. Power Deliv. 2016, Vol. 31 (2360–2369).

[4]. N. R. Watson & A. Farzanehrafat (2014): Three-phase transient state estimation algorithm for distribution systems. IET Gener. Transm. Distrib. 2014, Vol. 8 (1656–1666).

[5]. I. Sadeghkhani, M. E. Hamedani Golshan, A. Mehrizi-Sani, J. M. Guerrero, A. Ketabi (2018): Transient Monitoring Function–Based Fault Detection for Inverter-Interfaced Microgrids. IEEE Trans. Smart Grid 2018, Vol. 9 (2097–2107).

[6]. J. Furgał (2020): Influence of lightning current model on simulations of overvoltage in high voltage overhead transmission systems. Energies 2020, Vol. 13, 296.

[7]. M. Hamed & D. Ismail (1988): Correlation of switching overvoltage over transposed and non-transposed transmission lines, Open Access, Article ID 058670, Received 30 Jul 1986 Vol. 13, https://doi.org/10.1155/1988/58670 https://www.hindawi.com/journals/apec/1988/058670

[8]. L. V. Bewley, (1931): Traveling waves on transmission systems. Trans. Am. Inst. Electr. Eng. 1931, Vol. 50 (532–550).

[9]. J. A. Martinez, & F. Castro-Aranda (2005): Tower modeling for lightning analysis of overhead transmission lines. In Proceedings of the IEEE Power Engineering Society General Meeting, San Francisco, CA, USA, 12–16 June 2005, (1212–1217).

[10]. Asif, M. Lee, H. Y. Khan, U. A. Park, K. H. B.W. Lee (2018): Analysis of transient behavior of mixed high voltage dc transmission line under lightning strikes. IEEE Access 2018, Vol. 7 (7194–7205).

[11]. P. Paranavithana, S. Perera, R. Koch, & Z. Emin (2009): Global voltage unbalance in MV networks due to line asymmetries, IEEE Trans. Power Deliv. 2009, Vol. 24 (2353–2360).

[12]. Patrick Krkotić, Queralt Gallardo, Nikki Tagdulang, Montse Pont, & Juan M. O'Callaghan (2021): Algorithm for Resonator Parameter Extraction From Symmetrical and Asymmetrical Transmission

Responses, ID TMTT-2020-12-1418.R2, Submitted March 22nd, 2021, CERN Supported, Grants FCC-GOV-CC-0210 (KE4945/ATS), & FCC-GOV-CC-0209 (KE4946/ATS), UPC funding of Excellence María de Maeztu MDM2016-0600. NT acknowledges MSCA-COFUND-2016-754397 for PhD grant.

[13]. Diego Bellan (2020): Clarke Transformation Solution of Asymmetrical Transients in Three-Phase Circuits, Received: 25 Sep. 2020; Accepted: 6 Oct. 2020; Published: 8 Oct. 2020.

[14]. L. S. Martins, J. F. Martins, V. F. Pires, & C. M. Alegria (2005): The application of neural networks and Clarke-Concordia transformation in fault location on distribution power systems. Proceeding of the IEEE/PES Trans. & Distribution Conf. & Exhibition, Yokohama, Japan, 6–10 Oct. 2005 (2091–2095).

[15]. M. Asif, H. Y. Lee, K. H. Park A. Shakeel & B. W. Lee (2019): Assessment of overvoltage and insulation coordination in mixed HVDC transmission lines exposed to lightning strikes. Energies 2019, Vol. 12, 4217.